Pinned Scroll Rings in an Excitable System

Zulma A. Jiménez, Bradley Marts, and Oliver Steinbock
Department of Chemistry and Biochemistry, Florida State University, Tallahassee, Florida 32306-4390, USA
(Received 10 April 2009; published 15 June 2009)

Three-dimensional spiral waves in the Belousov-Zhabotinsky reaction are pinned to unexcitable heterogeneities. This pinning can prevent the collapse of scroll rings even if the heterogeneity does not extend along the entire wave filament. In the latter case, frequency differences create stationary gradients in the rotation phase. These twist patterns and their frequencies agree with algebraic solutions of the forced Burgers equation revealing insights into the phase coupling of scroll waves.

DOI: 10.1103/PhysRevLett.102.244101 PACS numbers: 05.45.−a, 82.40.Ck, 82.40.Qt

Coupled, nonlinear oscillators show intriguing complexities and are relevant to numerous technological and biomedical problems. Examples include Josephson junctions, electrochemical reactions, associative memory models [1], and scroll waves in excitable media. The latter structures are three-dimensional continua of spirals that rotate around one-dimensional space curves (called ''filaments'') with a characteristic local frequency and phase. As for many other coupled oscillators, these quantities change in time according to the oscillators' connectivity and coupling. In the case of filaments, the entire system also evolves due to curvature- and phase-controlled self-motion. In addition to this intriguing feature, scroll waves are important solutions of many reaction-diffusion models and have been observed in systems as diverse as the Belousov-Zhabotinsky (BZ) reaction, cellular slime molds, and cardiac tissue [2].

Filament motion has been carefully analyzed by several authors [3], and progress is also being made towards understanding turbulent states that arise from negative filament tension [4]. However, the specific nature of the underlying oscillator coupling and the resulting phase dynamics are not well studied. Theoretical analyses suggest a description in terms of Burgers' equation [5]. This nonlinear diffusion equation has been applied to a variety of problems in interface growth, acoustics, traffic flow, and cosmology, but a clear experimental demonstration of its applicability to excitable systems has remained elusive [6,7]. The sparseness of experimental data is partly due to the fact that phase gradients along the filament, called ''twist,'' are unstable in homogeneous systems [8].

A promising alternative is to generate stationary twist patterns by pinning scroll waves to heterogeneities [9]. Such a situation also has biomedical relevance since cardiac experiments have shown pathological rotors of electric activity anchored to inactive regions, such as arteries or connective tissue [10]. For two-dimensional excitable systems, intentional vortex pinning has been accomplished using laser beams, patterned catalyst membranes, and lithographically structured reactors [11]. However, in three-dimensional media, most of these techniques cannot be applied. In this Letter, we describe the first, well-controlled experiments that demonstrate scroll wave pinning. The stationary twist profiles of the pinned vortices are found to agree with solutions of Burgers' equation and allow the measurement of the system's linear and nonlinear diffusion constants.

Our experiments use the ferroin-catalyzed BZ reaction. The lower 4.0 mm of the disk-shaped medium (diameter 9 cm) are contained in an agrose gel (0.8% weight/volume), while the upper 4.0 mm are liquid solution. The initial reactant concentrations are constant throughout these two layers and equal: $[H_2SO_4] = 0.16$ mol/L, $[NaBrO_3] = 0.04$ mol/L, [malonic acid] $= 0.04$ mol/L, and $[Fe(phen)_3SO_4] = 0.5$ mmol/L. Scroll waves are created in two steps. First, an expanding spherical wave is initiated by contacting a silver wire to the gel-liquid interface for ca. 15 s. Then, the system is swirled rapidly causing mixing of the solution, which erases the wave in the upper phase. Once fluid motion ceases, the rim of the unaffected, gel-bound wave begins to curl spontaneously into the liquid phase, thus, nucleating the desired scroll wave. The filament is a near circular loop parallel and in close vicinity to the gel-solution interface. The wave patterns appear as blueish bands on a red background due to a color difference between the oxidized and reduced form of the catalyst. They are monitored with a video camera mounted above the system.

Because of their loop-shaped filament, the latter wave patterns are called scroll rings [see Fig. 1(a)]. As expected from earlier studies, the filament shrinks at a rate proportional to its curvature causing the annihilation of the vortex structure [12]. These striking dynamics constitute an unambiguous test case for the pinning of the vortex as the fully pinned scroll ring should not collapse. We attempt vortex pinning by (1) placing a chemically inert O ring onto the solution covered gel surface and (2) initiating the nonrotating wave at its center. The ring is made of the fluoropolymer viton (ORI Co.). It is well described by a torus generated from a disk of radius r revolving around a circle of radius $R = 3.1$ mm.

Figures 1(b) and 1(c) are representative space-time plots of a free and a pinned scroll ring, respectively. Filament

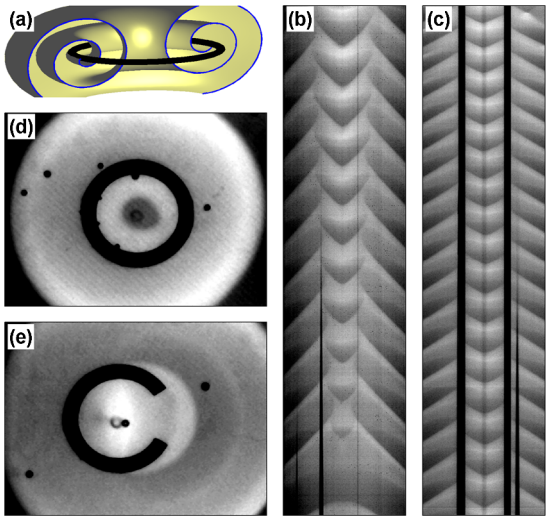

FIG. 1 (color online). (a) Sketch of a scroll ring rotating around a thin, ring-shaped obstacle. (b), (c) Space-time plots of a free, collapsing, and a pinned scroll ring, respectively. The horizontal axes span 15 mm. Time evolves in downward direction covering 70 min in (b) and 130 min in (c). (d), (e) Top view of a scroll ring pinned to a full O ring and a cut O ring ($\vartheta = 60°$), respectively. Field of view: 14×10 mm^2.

detection from such plots was first used by Pertsov *et al.* [13]. They are stacks of absorption profiles in which time evolves in downward direction. The profiles are measured along lines through the center of the scroll ring and cut the filament twice. In Figs. 1(b) and 1(c), these crossing points appear as regions that generate left and rightward propagating waves in an alternating fashion. The distance between the points equals the diameter ($2R(t)$) of the filament loop. In Fig. 1(b), this diameter decreases in time and the filament disappears after approximately 60 min. Our measurements confirm that this decay obeys the expected dependence $R(t)^2 = R(0)^2 - 2\alpha t$ [12] with a filament tension of $\alpha = 7.3 \times 10^{-5}$ cm^2/s. The thin but widening, dark lines in both space-time plots are due to small CO_2 bubbles and should not be mistaken with the O ring. More importantly, in Fig. 1(c), this contraction of the filament loop is absent, which strongly suggests that the scroll ring has been pinned successfully to the obstacle. Systematic variations of the obstacle thickness r between 2.6 and 3.6 mm reveal that the wave frequency decreases with increasing r (data not shown). This finding is consistent with circumference-controlled rotation periods known from two-dimensional systems [14] and, thus, provides additional evidence for the successful pinning of the scroll waves.

Figure 1(d) shows a top-view snapshot of a pinned scroll ring [15]. This typical example illustrates that the phase of the wave pattern has essentially no azimuthal dependence. Consequently, spiral rotation around the obstacle is synchronized, and the wave pattern is untwisted. In a small number of experiments, the initial pattern was mildly desynchronized or even had small segments of its filament detached; however, even those structures quickly approached the fully pinned and synchronized state.

The latter observations suggest that scroll wave pinning is a robust phenomenon. Perhaps even more surprisingly, we find that scroll rings can also be anchored to obstacles that do not allow for complete pinning. Notice that filaments can only end at boundaries and then must do so in pairs with complementary rotation direction [9]. Figure 1(e) shows a snapshot of an experiment with an O ring from which a large segment was cut out. In this case, most of the scroll wave rotates around the obstacle, but a smaller segment evolves freely within the gap. Systematic variations of the cut angle ϑ reveal that scroll collapse is prevented for $\vartheta \leq 180°$. Obstacles with larger cut angles are nonetheless effective in pinning the scroll ring locally; however, they fail to avert the collapse of the free filament towards the obstacle and cannot stop the resulting vortex annihilation.

In the following, we discuss the case of partially pinned but noncollapsing scroll waves. The example in Fig. 1(e) shows that the rotation phase lacks azimuthal synchronization. Movies of such experiments reveal wave motion that starts in the gap region and then rapidly moves along the upper and lower half of the obstacle. To analyze this motion and the corresponding twist pattern, we measure the excitation phase ϕ along a circle tracing the outer edge of the obstacle. The corresponding phase profiles are parameterized according to the circle's azimuth θ where $\theta = 0$ is the center of the gap. Our data show that the phase profiles $\phi(\theta)$ approach near-stationary solutions within several rotation periods of the pattern. This process tends to be slower for thick rings than for thin ones. Figure 2 shows representative examples of the resulting phase pro-

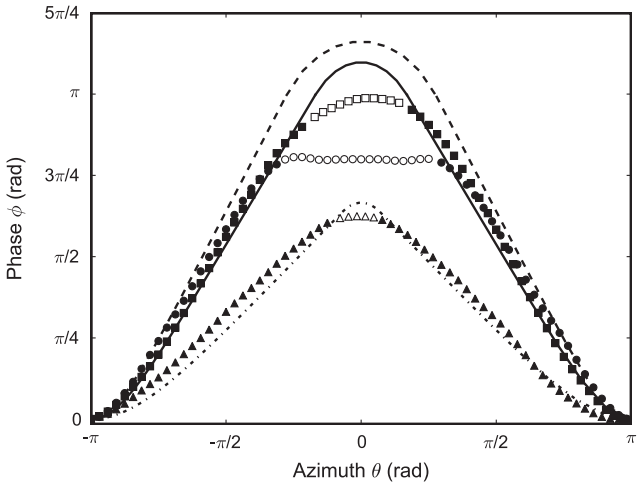

FIG. 2. Rotation phases of partially pinned scroll rings as a function of the azimuthal angle for three different cut angles. The gap in the O rings is centered around $\theta = 0$. Open and solid symbols distinguish between unpinned and pinned intervals, respectively. The curves graph the integrated, analytical solutions in Eqs. (3) and (4). The cut angles are $\vartheta = 25°$ (triangles, dotted), 60° (circles, continuous), and 101° (squares, dashed).

files for three different cut angles. Notice that the flanks of the curves are nearly linear indicating a constant twist of the scroll wave. The absolute value of this twist and the maximal phase variation increases with the cut angle.

We compare our experimental data to solutions of Burgers' equation. In terms of the phase and twist ($\tau = \phi_\theta$) dynamics on a ring, this equation can be written as [7]

$$\phi_t = \omega + c(\phi_\theta)^2 + D\phi_{\theta\theta}, \tag{1}$$

$$\tau_t = \omega_\theta + c\tau\tau_\theta + D\tau_{\theta\theta}, \tag{2}$$

where ω is the local spiral rotation frequency for an untwisted scroll wave and the subscripts t and θ indicate partial derivatives with respect to time and azimuthal angle, respectively. Notice that in a heterogeneous system, ω may depend on θ. The system-specific parameters c and D have units of frequency and differ from the conventional diffusion constants of the Burgers equation by a factor of $1/R^2$ where R is the ring radius.

In general, Eqns. (1) and (2) cannot be solved in closed form. However, for some $\omega(\theta)$, we can find solutions for the asymptotic state when $\phi_t = \Omega$ is constant. To describe the experimental situation, we approximate $\omega(\theta)$ as piecewise constant equalling the frequency of the free scroll wave within the gap and the frequency of the fully pinned scroll along the O ring. In the following, we distinguish these two intervals by using the subscript "p" for the pinned region and "u" for the (unpinned) gap region. Then, we are interested in the stationary solutions of Eqn. (2) where $\omega_\theta = 0$. Moreover, these solutions must fit the symmetry of the O ring and match at the boundary between intervals "p" and "u." These solutions are

$$\tau_p(\theta) = A\frac{D}{c}\tanh[A(\pi - |\theta|)], \tag{3}$$

$$\tau_u(\theta) = -B\frac{D}{c}\tan(B\theta). \tag{4}$$

The latter equations describe twisted scroll waves with constant rotation frequencies, $\Omega_p = \omega_p + A^2D^2/c$ and $\Omega_u = \omega_u - B^2D^2/c$, where ω_p and ω_u are the frequencies of the untwisted pinned and free scrolls, respectively.

Notice that the phase has to be differentiable and its derivative (the twist) continuous, particularly at the boundary between the pinned filament and the free filament. This constraint, along with the condition that every point on the wave rotates with the same frequency $\Omega_p = \Omega_u$, yields the following criteria for the constants A and B:

$$A\tanh[A(\pi - \vartheta/2)] = B\tan(B\vartheta/2), \tag{5}$$

$$\omega_u - \omega_p = (B^2 + A^2)\frac{D^2}{c}, \tag{6}$$

which, for given values of c and D, can be solved numerically for A and B. Notice that $B < \pi/\vartheta$ to rule out singularities in $\tau_p(\theta)$ and A, $B > 0$ without loss of generality.

This analysis yields best agreement with our experimental data for $c = 4.8 \times 10^{-4}$ s^{-1} and $D = 3.5 \times 10^{-4}$ s^{-1}, which are used throughout this Letter and correspond to diffusion coefficients of 4.7×10^{-5} cm^2/s and 3.5×10^{-5} cm^2/s, respectively ($R = 3.1$ mm). For instance, the continuous curves for the phase in Fig. 2 are based on the integrated expressions for twist in Eqs. (3) and (4) and agree well with the measured phase profiles along the obstacle. Notice that we can calculate the slope of the phase ϕ in the range where it is nearly linear. This slope corresponds to the largest absolute value of the twist, $\tau_{\max}$, which in our measurements is approximately the value of $|\tau|$ at $\theta = \pm\vartheta/2$:

$$\tau_{\max} \approx AD/c = \sqrt{\frac{\Omega - \omega_p}{c}}. \tag{7}$$

Within the gap region, the theoretical curves show larger deviations from the experimental data. We suggest that these deviations stem primarily from our simple assumption that the filament traces the O ring's outer perimeter within the gap region. However, our experiments show that the filament might actually be better described by a straight line which is shifted towards the inner perimeter of the obstacle. For the sake of clarity and brevity, possible corrections are not discussed here. Moreover, the detailed wave dynamics in very close vicinity to the end points of the obstacle are poorly understood and might not be adequately described by a reduction to a one-dimensional filament.

To further characterize the partially pinned scroll rings, we measured their angular frequency as a function of the cut angle ϑ. As shown in Fig. 3, the frequency increases with increasing gap size in a sigmoidal fashion. Notice that the values for $\vartheta = 0$ and 2π equal the frequencies of the

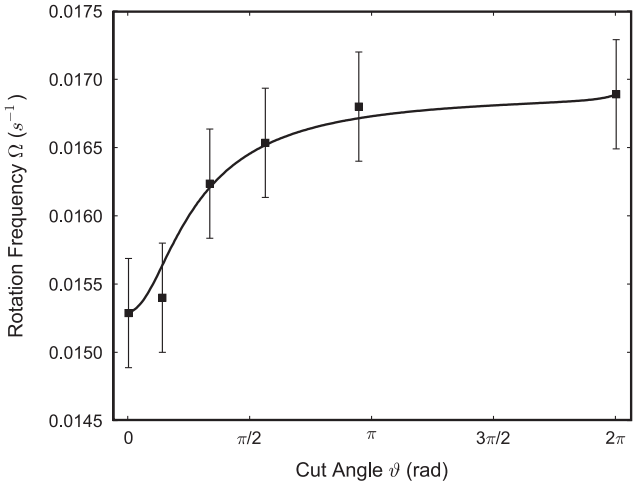

FIG. 3. Angular rotation frequency of partially pinned scroll rings as a function of the obstacle's gap size. Notice that $\vartheta = 0$ and 2π are the fully pinned and unpinned cases, respectively. The continuous curve is the theoretical prediction in terms of Burgers' equation.

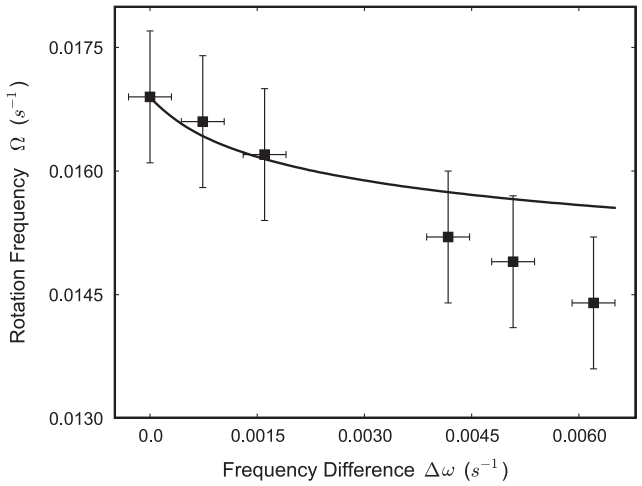

FIG. 4. Angular rotation frequency of partially pinned scroll rings as a function of the frequency difference $\Delta\omega = \omega_u - \omega_p$ for $\vartheta \approx 55°$. This difference is increased by increasing the thickness r of the O ring at constant ω_u. The continuous line is the theoretical prediction in terms of Burgers' equation.

fully pinned and unpinned (i.e., free) scroll ring, respectively. Each experiment was repeated at least three times, and error bars represent standard deviations. The continuous curve in Fig. 3 is calculated from the equation for Ω_p (or equivalently Ω_u) given above. We find excellent agreement with the experimental data.

Qualitatively, the results in Fig. 3 can be understood by considering the fast in-gap rotation as a "motor" that twists the slower, pinned part of the scroll ring. This process is limited by the reaction-diffusion-controlled characteristics of the system and results in a stationary, twisted rotation pattern. The strength of the twisting action, however, does not only depend on the gap width but also on the frequency difference $\Delta\omega$ between the freely rotating and fully pinned scroll ring. In our experiments, we vary this difference by changing the width r of the employed O ring, which changes the value of ω_p while keeping ω_u constant. Figure 4 shows the stationary rotation frequency of the scroll ring as a function of $\Delta\omega$ for a constant cut angle of approximately 55°. Notice that large values of $\Delta\omega$ correspond to thick obstacles. The measured values of Ω (Fig. 4) decrease in a nearly linear fashion with $\Delta\omega$. The continuous curve is calculated based on Eqs. (3)–(6). It is in good agreement with the experimental data, but slightly overestimates the observed frequencies at large $\Delta\omega$. These deviations might be due to the aforementioned repositioning of the filament in the gap region, which is more pronounced for large r. Furthermore, it might also suggest that phase coupling [Eqs. (1) and (2)] involves higher order terms in τ that are currently not considered. Unfortunately, it is difficult to study patterns with even larger frequency differences because such structures are readily enslaved by other (spontaneously forming) vortices of higher frequency.

In conclusion, we have presented concrete experimental evidence that scroll wave can be pinned to solid obstacles. We believe that this pinning is a universal feature of heterogeneous excitable media and that it could greatly affect the dynamics of vortices in biological systems where inhomogeneities are abundant. In addition, we have demonstrated that stable, partial pinning is possible causing twisted patterns that are stationary solutions of Burgers' equation. Future studies should explore the processes of filament capture, possible limitations of scroll pinning, and filament unpinning.

This material is based upon work supported by the National Science Foundation under Grant No. 0513912.

[1] J. A. Acebron, L. L. Bonilla, C. J. P. Vicente, F. Ritort, and R. Spigler, Rev. Mod. Phys. **77**, 137 (2005); I. Z. Kiss, C. G. Rusin, H. Kori, and J. L. Hudson, Science **316**, 1886 (2007).

[2] A. T. Winfree, Science **181**, 937 (1973); O. Steinbock, F. Siegert, S. C. Müller, and C. J. Weijer, Proc. Natl. Acad. Sci. U.S.A. **90**, 7332 (1993); F. H. Fenton, E. M. Cherry, H. M. Hastings, and S. J. Evans, Chaos **12**, 852 (2002).

[3] B. Echebarria, V. Hakim, and H. Henry, Phys. Rev. Lett. **96**, 098301 (2006).

[4] J. P. Keener, Physica D (Amsterdam) **31**, 269 (1988); J. Davidsen, M. Zhan, and R. Kapral, Phys. Rev. Lett. **101**, 208302 (2008).

[5] J. P. Keener and J. J. Tyson, SIAM Rev. **34**, 1 (1992); D. Margerit and D. Barkley, Chaos **12**, 636 (2002).

[6] A. M. Pertsov, R. R. Aliev, and V. I. Krinsky, Nature (London) **345**, 419 (1990).

[7] B. Marts, T. Bánsági, Jr., and O. Steinbock, Europhys. Lett. **83**, 30010 (2008).

[8] A. S. Mikhailov, A. V. Panfilov, and A. N. Rudenko, Phys. Lett. A **109**, 246 (1985).

[9] M. Vinson, S. Mironov, S. Mulvey, and A. Pertsov, Nature (London) **386**, 477 (1997); A. M. Pertsov, M. Wellner, M. Vinson, and J. Jalife, Phys. Rev. Lett. **84**, 2738 (2000).

[10] J. M. Davidenko, A. M. Pertsov, R. Salomonsz, W. Baxter, and J. Jalife, Nature (London) **355**, 349 (1992); K. Agladze, M. W. Kay, V. Krinsky, and N. Sarvazyan, Am. J. Physiol, Heart Circ. Physiol. **293**, H503 (2007).

[11] O. Steinbock and S. C. Müller, Phys. Rev. E **47**, 1506 (1993); O. Steinbock, P. Kettunen, and K. Showalter, Science **269**, 1857 (1995); B. T. Ginn and O. Steinbock, Phys. Rev. Lett. **93**, 158301 (2004).

[12] T. Bánsági, Jr. and O. Steinbock, Phys. Rev. Lett. **97**, 198301 (2006).

[13] A. Pertsov, M. Vinson, and S. C. Müller, Physica D (Amsterdam) **63**, 233 (1993).

[14] B. T. Ginn and O. Steinbock, Phys. Rev. E **72**, 046109 (2005).

[15] See EPAPS Document No. E-PRLTAO-103-014927 for movies of typical experiments. For more information on EPAPS, see http://www.aip.org/pubservs/epaps.html.